

## Rapid low-temperature consolidation of nanocrystalline Co-ZrO<sub>2</sub> composite by pulsed current activated sintering and its mechanical properties

In-Jin Shon\* and Na-Ra Park

Division of Advanced Materials Engineering, the Research Center of Advanced Materials Development, Chonbuk National University, 664-14 Deokjin-dong 1-ga, Deokjin-gu, Jeonju, Jeonbuk 561-756, Republic of Korea

Nanopowders of Co and ZrO<sub>2</sub> were synthesized from Co<sub>3</sub>O<sub>4</sub> and Zr by high energy ball milling. The powder sizes of Co and ZrO<sub>2</sub> were 10 nm and 16 nm, respectively. Highly dense nanostructured 3Co-2ZrO<sub>2</sub> composite was consolidated by pulsed current activated sintering method within 3 minutes from the mechanically synthesized powders (Co-ZrO<sub>2</sub>) and horizontal milled Co<sub>3</sub>O<sub>4</sub> + Zr powders under the 1 GPa pressure. The grain sizes of Co and ZrO<sub>2</sub> in the composite were calculated. The average hardness and fracture toughness values of nanostructured 3Co-2ZrO<sub>2</sub> composite were investigated.

**Key words:** Rapid sintering, Composite, Nanomaterial, Mechanical properties, Co-ZrO<sub>2</sub>.

### Introduction

The continuous increase in the performance requirement of materials for aerospace and automotive applications have lead to development of several structural composite materials. Among these, metal matrix composites refer to a kind of material in which rigid ceramic reinforcements are embedded in a ductile metal or alloy matrix. Metal matrix composites combine metallic properties (ductility and toughness) with ceramic characteristics (high strength and modulus), leading to greater strength in shear and compression and to higher service temperature capabilities. The attractive physical and mechanical properties that can be obtained with metal matrix composites, such as high specific modulus, strength-to weight ratio, fatigue strength, and temperature stability and wear resistance, have been documented extensively [1].

ZrO<sub>2</sub> has a density of 5.98 g · cm<sup>-3</sup>, a Young's modulus of 210 GPa, excellent oxidation resistance and good high-temperature mechanical properties [2]. Co has a density of 8.30 g · cm<sup>-3</sup>, a Young's modulus of 209 GPa and good fracture toughness [3]. Hence, microstructure consisting of Co and ZrO<sub>2</sub> may be able to satisfy the good mechanical properties requirements of successful structural material.

Traditionally, discontinuously reinforced metal matrix composites have been produced by several processing routes such as powder metallurgy, spray deposition mechanical alloying, various casting techniques and SHS (self-propagating high temperature synthesis). All these techniques are based on the addition of ceramic

reinforcements to the matrix materials which may be in molten or powder form. One of all these techniques, high energy ball milling and mechanical alloying of powder mixtures, were reported to be efficient techniques for the preparation of nano-crystalline metals and alloys, which is a combination of mechanical milling and chemical reactions [4].

Nanocrystalline materials, as advanced engineering materials, have received much attention due to their improved physical and mechanical properties. In recent days, nanocrystalline powders have been developed by co-precipitation, the thermochemical and thermomechanical process named as the spray conversion process (SCP), and high energy milling [5-7]. The grain size in sintered materials, however, becomes much larger than that in pre-sintered powders due to a fast grain growth during conventional sintering process. Therefore, controlling grain growth during sintering is one of the keys to the commercial success of nanostructured materials. In this regard, the pulsed current activated sintering method which can make dense materials within 2 min, has been shown to be effective in achieving this goal [8].

The purpose of this work is to produce nanopowders of Co, ZrO<sub>2</sub> and dense nanocrystalline Co-ZrO<sub>2</sub> composite within 2 minutes from mechanically synthesized powders (Co-ZrO<sub>2</sub>) and horizontal milled Co<sub>3</sub>O<sub>4</sub> + Zr powders using this pulsed current activated sintering method and to evaluate its grain size and mechanical properties (hardness and fracture toughness).

### Experimental Procedure

Powders of 99.5% Co<sub>3</sub>O<sub>4</sub> (< 10 μm, Aldrich, Inc) and 99.5% pure Zr (-325 mesh, Sejong, Inc) were used as a starting materials. The Co<sub>3</sub>O<sub>4</sub> powder and Zr powder have angular and irregular shape, respectively, as shown

\*Corresponding author:  
Tel : +82 63 270 2381  
Fax: +82 63 270 2386  
E-mail: ijshon@chonbuk.ac.kr

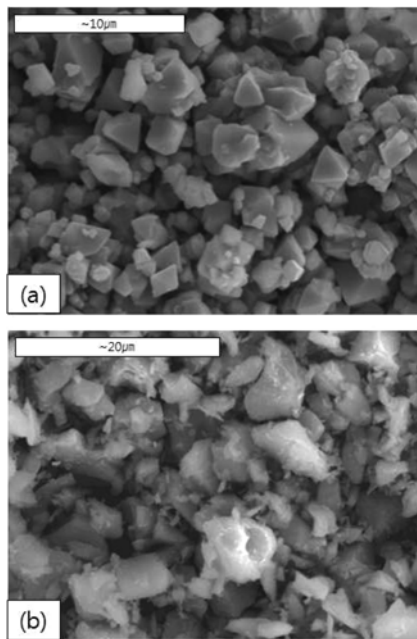


**Fig. 1.** Scanning electron microscope image of raw materials : (a) Co<sub>3</sub>O<sub>4</sub>, (b) Zr.

in Fig. 1. Co<sub>3</sub>O<sub>4</sub> and 2 Zr powders were mixed by two type methods. Firstly, the powders were milled in a high-energy ball mill, Pulverisette-5 planetary mill at 250 rpm and for 10 h. Tungsten carbide balls (8.5 mm in diameter) were used in a sealed cylindrical stainless steel vial under argon atmosphere. The weight ratio of ball-to-powder was 30 : 1. Secondly, the powders were mixed in polyethylene bottles using zirconia balls with ethanol and it was performed at a horizontal rotation velocity of 250 rpm for 10 h. The grain size of ZrO<sub>2</sub> was calculated by Suryanarayana and Grant Norton's formula [9] :

$$B_r (B_{crystalline} + B_{strain}) \cos\theta = k \lambda / L + \eta \sin\theta \quad (1)$$

where  $B_r$  is the full width at half-maximum (FWHM) of the diffraction peak after instrumental correction;  $B_{crystalline}$  and  $B_{strain}$  are FWHM caused by small grain size and internal stress, respectively;  $k$  is constant (with a value of 0.9);  $\lambda$  is wavelength of the X-ray radiation;  $L$  and  $\eta$  are grain size and internal strain, respectively; and  $\theta$  is the Bragg angle. The parameters  $B$  and  $B_r$  follow Cauchy's form with the relationship:  $B = B_r + B_s$ , where  $B$  and  $B_s$  are FWHM of the broadened Bragg peaks and the standard sample's Bragg peaks, respectively.

After milling, the mixed powders were placed in a WC die (outside diameter, 40 mm; inside diameter, 5 mm; height, 40 mm) and then introduced into the pulsed current activated sintering system made by Eltek in South Korea shown schematically in Fig. 2. The four major stages in the sintering are as follows. The system was evacuated (stage 1) and a uniaxial pressure of 1 GPa was applied (stage 2). A pulsed current (on time; 20  $\mu$ s, off time; 10  $\mu$ s) was then

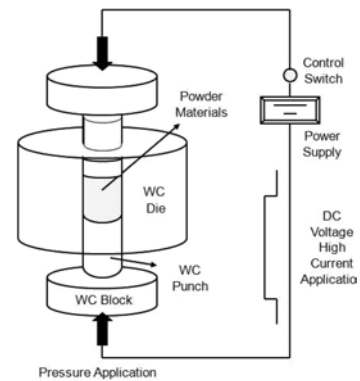


**Fig. 2.** Schematic diagram of the pulsed current activated sintering apparatus.

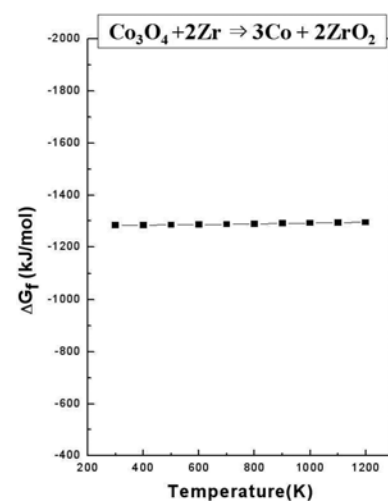


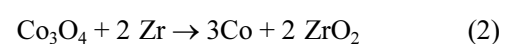
**Fig. 3.** Temperature dependence of the Gibbs free energy variation by interaction of Co<sub>3</sub>O<sub>4</sub> with 2 Zr.

activated and maintained to 670 °C with heating rate of 300 °C/min and then turned off without holding time (stage 3). The temperatures were measured using a pyrometer focused on the surface of the WC die. At the end of the process, the sample was cooled to room temperature (stage 4). The process was carried out under a vacuum of 5.33 Pa.

The relative densities of the sintered sample were measured by the Archimedes method. Microstructural information was obtained from product samples which were polished. Compositional and micro structural analyses of the products were made through X-ray diffraction (XRD) and scanning electron microscopy (SEM) with energy dispersive X-ray analysis (EDAX). Vickers hardness was measured by performing indentations at load of 20 kg and a dwell time of 15 s on the sintered samples.

## Results and Discussion

The interaction between Co<sub>3</sub>O<sub>4</sub> and 2 Zr, i.e.,



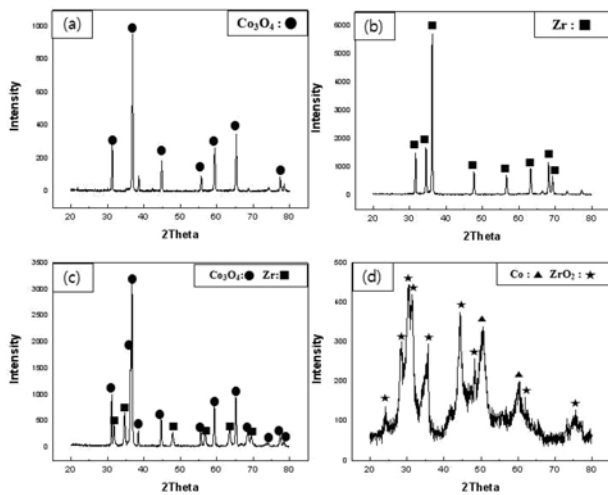


Fig. 4. XRD patterns of raw materials: (a)  $\text{Co}_3\text{O}_4$ , (b) Zr, (c) horizontal milled powders and (d) mechanically milled powders.

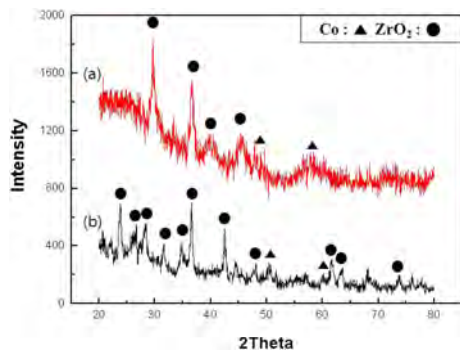


Fig. 5. XRD patterns of Co-ZrO<sub>2</sub> composite sintered from (a) high energy ball milled powders and (b) horizontal milled powders.

is thermodynamically feasible as shown in Fig. 3.

The X-ray diffraction pattern of horizontal milled powder and mechanically high energy ball milled powders from raw powders are shown in Fig. 4(c) and 4(d), respectively. Co-ZrO<sub>2</sub> was not synthesized during the horizontal rotation ball milling in ethanol, but synthesized during high energy ball milling. From above results, solid replacement reaction completely occurs during the high energy ball milling. The full width at half-maximum (FWHM) of the diffraction peak is broad due to refinement of powder and strain. The average grain sizes of ZrO<sub>2</sub> measured by Suryanarayana and Grant Norton's formula were about 16 nm.

XRD patterns of the high-energy ball milled powder and the horizontal ball milled powder heated to 670 °C is shown in Fig. 5. Only Co and ZrO<sub>2</sub> peaks are detected. From X-ray patterns of Fig. 4(a) and Fig. 5(b), Co-ZrO<sub>2</sub> was synthesized from horizontal milled powder of Co<sub>3</sub>O<sub>4</sub> and 2 Zr. Fig. 6 shows plot of  $B_r \cos \theta$  versus  $\sin \theta$  to calculate grain size of ZrO<sub>2</sub>. The structure parameters, i.e. the average grain sizes of ZrO<sub>2</sub> in composite sintered from horizontal milled powder and high energy ball milled powder obtained from X-ray data in Fig. 6 by Suryanarayana and Grant

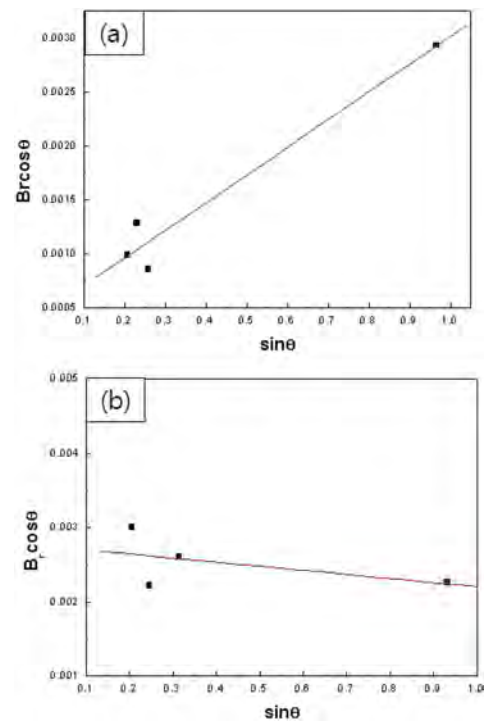


Fig. 6. Plot of  $B_r \cos \theta$  versus  $\sin \theta$  of ZrO<sub>2</sub> in composite sintered from (a) horizontal milled powders and (b) high energy ball milled powders.

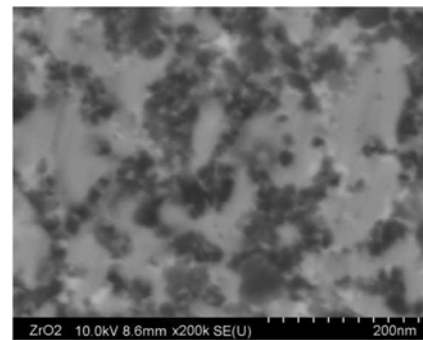
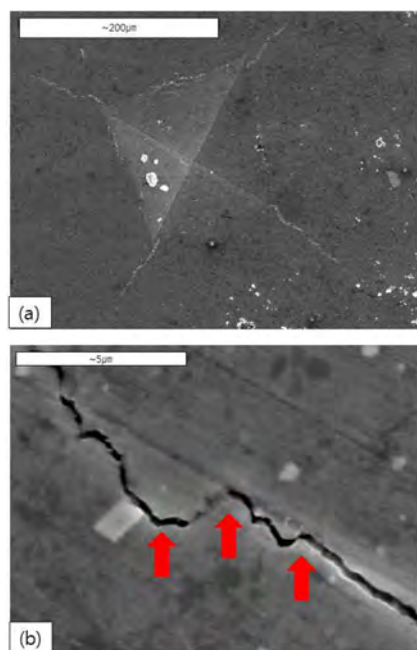


Fig. 7. FE-SEM images of Co-ZrO<sub>2</sub> composite sintered from high energy ball milled powders.

Norton's formula, are 174, 80 nm, respectively. And the relative density of the Co-ZrO<sub>2</sub> composites were 95% and 97%, respectively. It is considered that the average grain sizes of ZrO<sub>2</sub> in composite sintered from horizontal milled powder is higher than those from high energy ball milled powder because during the heating of horizontal milled powder, the gains growth of ZrO<sub>2</sub> occurs due to combustion synthesis. FE-SEM images of Co-ZrO<sub>2</sub> composite sintered at 670 °C from high energy ball milled powders are shown in Fig. 7. The composites consist of nanograins. It is considered that the reasons of high density of the composite obtained at low temperature are as follows. Firstly, the application of pressure during initial stage sintering adds another term to the surface energy driving force such the total driving force,  $F_D$ , is now [10]



**Fig. 8.** (a) Vickers hardness indentation and (b) median crack propagating in the Co-ZrO<sub>2</sub> composite sintered from high energy ball milled powders.

$$F_D = \gamma + (P_a r / \pi), \quad (3)$$

where  $\gamma$  is the surface energy,  $P_a$  is the applied pressure, and  $r$  is the radius of the particle. The effect of pressure on the densification of TiO<sub>2</sub> during high-frequency induction heated sintering was investigated by Shon et al. [11]. A significant increase in the relative density was observed as the pressure was increased from about 60 to 100 MPa for sintering at 800 °C. Secondly, The role of the current (resistive or inductive) in sintering and or synthesis has been focus of several attempts aimed at providing an explanation to the observed enhancement of sintering and the improved characteristics of the products. The role played by the current has been variously interpreted, the effect being explained in terms of fast heating rate due to Joule heating, the presence of plasma in pores separating powder particles, and the intrinsic contribution of the current to mass transport [12-15].

Vickers hardness measurements were made on polished sections of the 3 Co-2 ZrO<sub>2</sub> composite using a 20 kg<sub>f</sub> load and 15 sec dwell time. The calculated hardness value of 3 Co-2 ZrO<sub>2</sub> composite sintered 670 °C from horizontal milled powders and high energy ball milled powders were 4, 5.6 GPa, respectively. This value represents an average of five measurements. Indentations with large enough loads produced median cracks around the indent. The length of these cracks permits an estimation of the fracture toughness of the material. From the length of these cracks, fracture toughness values can be determined using by Anstis et al. [16] is

$$K_{IC} = 0.016 (E/H)^{1/2} \cdot P/C^{3/2} \quad (4)$$

where  $E$  is Young's modulus,  $H$  the indentation hardness,  $P$  the indentation load, and  $C$  the trace length of the crack measured from the center of the indentation. The modulus was estimated by the rule of mixtures for the 0.69 volume fraction of ZrO<sub>2</sub> and the 0.31 volume fraction of Co using  $E(\text{ZrO}_2) = 207$  GPa [2] and  $E(\text{Co}) = 209$  GPa [3]. As in the case of hardness values, the toughness values were derived from the average of five measurements. The toughness values of composites obtained from horizontal milled powders and high energy ball milled are 8.5, 9 MPa · m<sup>1/2</sup>, respectively.

The hardness and fracture toughness of ZrO<sub>2</sub> are reported as 11.8 GPa and 6.5 MPa · m<sup>1/2</sup>, respectively [17]. The hardness of the 3 Co-2 ZrO<sub>2</sub> composite is lower than that of monolithic ZrO<sub>2</sub> but the fracture toughness is higher than that of ZrO<sub>2</sub> due to addition of ductile Co. Fig. 8 (a) shows Vickers indentation in the 3 Co-2 ZrO<sub>2</sub> composite sintered from high energy ball milled powders. One to three additional cracks were observed to propagate from the indentation corner. And crack propagated deflectively ( $\uparrow$ ) in Fig. 8(b).

## Conclusions

Nanopowders of ZrO<sub>2</sub> and Co were synthesized from Zr and Co<sub>3</sub>O<sub>4</sub> by high energy ball milling. The powder sizes of ZrO<sub>2</sub> was 16 nm. Using the pulsed current activated sintering method, the densification of nanostructured 3Co-2ZrO<sub>2</sub> composite was accomplished from mechanically synthesized powders and horizontal milled powders within duration of 3 minutes. The average grain sizes of ZrO<sub>2</sub> prepared by PCAS were lower than 100 nm. The average hardness and fracture toughness values obtained from mechanically synthesized powders and horizontal milled powders were 5.6, 4 GPa and 8.5, 9 MPa · m<sup>1/2</sup>, respectively. The fracture toughness of the Co-ZrO<sub>2</sub> composite is higher than that of monolithic ZrO<sub>2</sub>.

## Acknowledgment

“This research was supported by Basic Science Research Program through the National Research Foundation of Korea (NRF) funded by the Ministry of Education, Science and Technology (No. 2012001300) and following are results of a study on the “Leaders INdustry-university Cooperation” Project, supported by the Ministry of Education, Science & Technology (MEST).

## References

1. L. Ceschini, G. Minak, A. Morri, *Composites Science and Technology*, 66 (2006) 333-342.
2. S.G. Huang, *J. the European Ceramic Society* 27 (2007) 3269-3275.

3. [http://en.wikipedia.org/wiki/Elastic\\_properties\\_of\\_the\\_elements](http://en.wikipedia.org/wiki/Elastic_properties_of_the_elements) (data page).
4. S. Paris, E. Gaffet, F. Bernard, and Z.A. Munir, *Scripta Materialia* 50 (2004) 691-696.
5. Z. Fang, and J.W. Eason, *International Journal of Refractory Metals and Hard Materials* 13 (1995) 297-303.
6. A.I.Y. Tok, L.H. Luo, and F.Y.C. Boey, *Materials Science and Engineering: A* 383 (2004) 229-234.
7. H.S. Jun, I.Y. Ko, J.K. Yoon, J.M. Doh, K.T. Hong, S.H. Lee, In-Jin Shon, *Journal of Ceramic Processing Research* 12 (2011) 165-168.
8. H.S. Kang, I.Y. Ko, J.K. Yoon, J.M. Doh, K.T. Hong, I.J. Shon, *Metals and Materials International* 17 (2011) 57-62.
9. C. Suryanarayana, and M. Grant Norton, *X-ray Diffraction A Practical Approach*, Plenum Press, New York, 1998.
10. R.L. Coble, *J. Appl. Phys.* 41, (1970) 4798-4807.
11. H.C. Kim, H.K. Park, I.J. shon, I.Y. Ko, *Journal of Ceramic Processing Research* 7 (2006) 327-331.
12. Z. Shen, M. Johnsson, Z. Zhao and M. Nygren, *Spark Plasma Sintering of Alumina*, *J. Am. Ceram. Soc.* 85, (2002) 1921-1927.
13. J.E. Garay, U. Anselmi-Tamburini, Z.A. Munir, S.C. Glade and P. Asoka- Kumar, *Appl. Phys. Lett.* 85 (2004) 573-597.
14. J.R. Friedman, J.E. Garay. *U. Intermetallics* 12, (2004) 589-597.
15. J.E. Garay, J.E. Garay. U. Anselmi-Tamburini and Z.A. Munir, *Acta Mater.* 51 (2003) 4487-4495.
16. G.R. Anstis, P. Chantikul, B.R. Lawn, D.B. Marshall, *J. Am. Ceram. Soc.* 64 (1981) 533-538.
17. S.G. Huang, K. Vanmeensel, O. Van der Biest, J. Vleugels, *Journal of the European Ceramics Society* 27, 3269 (2007) 3269-3275.